IMPROVED PSEUDOLITE NAVIGATION USING C/N_0 MEASUREMENTS

Daniele Borio, Ciro Gioia

Institute for the Protection and Security of the Citizen, IPSC
EC Joint Research Centre, Ispra, Italy

ABSTRACT

The problem of indoor navigation using pseudolites is investigated and two different approaches, employing synchronous and asynchronous technologies, are considered. It is shown that synchronous pseudolite systems, commonly considered more accurate, seem to be unsuitable for deep indoor operations: in complex propagation environments, the synchronization required for metre level navigation is difficult to achieve and a different solution should be adopted.
The potential of asynchronous pseudolite systems is demonstrated and indoor navigation with metre level accuracy is obtained using C/N_0 measurements. In particular, the spectral characteristics of C/N_0 measurements are investigated and used to design a pre-filtering stage which, in turn, is employed to remove high-frequency noise. Pre-filtering significantly improves the navigation performance in harsh indoor environments.

***Index Terms*—** Global Navigation Satellite System (GNSS), Indoor Navigation, Pseudolites, Receiver Signal Strength Indicator (RSSI)

1. INTRODUCTION

Indoor navigation is a challenging task and requires solving several issues such as signal attenuation, multipath fading and measurement biases. Although local augmentation systems, such as pseudolites, have the potential to improve indoor navigation and extend the range of application of Global Navigation Satellite System (GNSS) services, several limitations are still present.
Pseudolites have been originally conceived to operate in a synchronous mode, i.e. all the pseudolites are synchronized to a common time scale and a pseudolite receiver generates pseudorange measurements in the same way as for GNSS signals. When pseudolites are synchronized to a GNSS time scale, direct integration of GNSS and pseudolite measurements can be performed. Although decimeter level accuracy can be achieved using a synchronous pseudolite system, this level of performance was demonstrated only for relatively friendly environments such as open-sky or in a large hangar [1]. When used indoors, multipath propagation, fading and other propagation effects can make synchronization impossible.
In this paper, the limitations of synchronous pseudolite systems have been investigated using a Commercial Off-the-Shelf (COTS) pseudolite system. Several tests were performed and different configurations were considered in deep indoor scenarios. Despite the significant efforts, it was not possible to achieve the synchronization required for metre level navigation and the limitations of this technology clearly emerged.
For this reason, an asynchronous approach has been adopted. In an asynchronous network, each pseudolite operates independently and the user position is no longer based on travel time measurements. In [2], a pseudolite positioning system based on Receiver Signal Strength (RSS) was suggested and metre level position accuracy was demonstrated in the corridor of a large office building. The approach proposed in [2] is further analyzed here and adapted to the COTS pseudolite system adopted for testing synchronous pseudolite navigation. The algorithm developed in [2] has been further refined and a pre-filtering stage has been introduced to improve location performance. Indoor navigation with metre level accuracy was achieved in different scenarios such as a large meeting room and a long corridor. Finally, the algorithm developed for asynchronous indoor navigation was implemented on an Android platform and real-time operations were demonstrated using a smartphone.
The remainder of this paper is organized as follows: the limitations of synchronous navigation systems are highlighted in Section 2 whereas the concept of asynchronous pseudolite positioning is discussed in Section 3. The impact of pre-filtering on Carrier-to-Noise density power ratio (C/N_0) measurements is analyzed in Section 4 and experimental results are detailed in Section 5. Finally, Section 6 concludes the paper.

2. LIMITATIONS OF SYNCHRONOUS INDOOR NAVIGATION

The COTS pseudolite system adopted for this work is composed of 6 pseudolites, a Master Control Station (MCS) and two modified GPS receivers able to collect GPS and pseudo-

This work has been partially supported by the European Commission in the framework of the EPCIP 2010 project (C.32253-2011 NFP - AWP CIPS 2010).

lite measurements [1, 3]. The MCS can synchronize the system either to GPS time or slave it to the clock of a single pseudolite denoted as Master Pseudolite (MPL). To this end, the MCS must have all the pseudolites in Line-Of-Sight (LOS): the MCS has to be able to accurately measure the pseudoranges of the different pseudolites and compare them with the actual distances stored in the MCS control software. Thus, multipath and other propagation errors have to be sufficiently small to achieve synchronization.

Several problems were encountered using the MCS: the MCS software performs several checks to verify the synchronization status. If the checks fail the process restarts without achieving even partial results. This was the case when the pseudolite system was installed in a deep indoor environment: using the MCS it was not possible to achieve the synchronization level required.

In order to overcome this issue and analyze measurement errors, a *relative positioning* approach was implemented. Two u-blox LEA-6T GPS devices were used as reference and rover receivers, respectively. The basic principle behind this approach is that reference and rover receivers are able to provide pseudorange measurements which can be modeled as

$$\begin{aligned}\rho_{rov,i} &= d_{rov,i} + b_{rov} + b_{pl,i} + \eta_{rov,i} \\ \rho_{ref,i} &= d_{ref,i} + b_{ref} + b_{pl,i} + \eta_{ref,i}\end{aligned} \tag{1}$$

where $d_{rov,i}$ and $d_{ref,i}$ are the geometric distances between rover/reference receivers and the ith pseudolite. b_{rov} and b_{ref} are the clock biases of the rover and reference receivers and $b_{pl,i}$ is the clock bias of the ith pseudolite.. $b_{pl,i}$ is the synchronization error which should be compensated for by the MCS and is specific of each pseudolite. $\eta_{rov,i}$ and $\eta_{ref,i}$ are residual unmodeled errors. The synchronization error, b_{pl_i}, can be removed by considering single pseudorange differences:

$$\begin{aligned}\Delta\rho_i &= \rho_{rov,i} - \rho_{ref,i} \\ &= d_{rov,i} - d_{ref,i} + b_{rov} - b_{ref} + \eta_{rov,i} - \eta_{ref,i}.\end{aligned} \tag{2}$$

Finally, using the geometric distance between the reference receiver and the ith pseudolite, it is possible to construct new measurements free of pseudolite synchronization errors:

$$\bar{\rho}_i = \Delta\rho_i + d_{ref,i} = d_{rov,i} + \Delta b + \Delta\eta_i \tag{3}$$

where $\Delta b = b_{rov} - b_{ref}$ and $\Delta\eta_i = \eta_{rov,i} - \eta_{ref,i}$. Note that (3) has the same functional form of the pseudoranges adopted for GNSS positioning [4] and in particular a single clock bias term, Δb, is present. This term is common to all the pseudolite measurements and can be estimated by adding it as unknown in the navigation solution. This is the same principle adopted by commercial GNSS receivers.

Note that the principle described above is valid only if the reference and rover receivers are accurately synchronized, i.e., if their measurements are generated and time-tagged using the same time reference. For this reason, two methodologies were adopted. In the first case, a specific pseudolite, named MPL, was turned on before all the other elements of the network. Additional pseudolites were activated only after that reference and rover receivers used the MPL signal for the measurement generation and time-tagging. Alternatively, when the receivers were able to determine a position fix using GPS, GPS time was adopted.

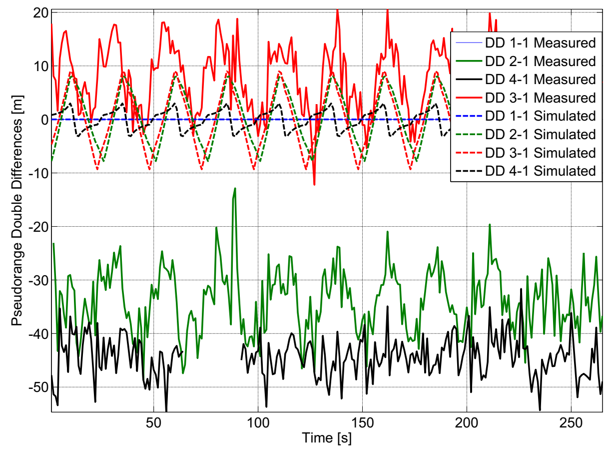

Fig. 1. Double pseudorange differences computed from the measurements collected from the four pseudolites using two LEA-6T u-blox receivers.

Despite these efforts, it was not possible to compute valid position fixes employing the measurements generated using (3). The problem was investigated considering double pseudorange differences

$$\nabla\Delta\rho_{i,j} = \bar{\rho}_i - \bar{\rho}_j. \tag{4}$$

Measured and simulated double pseudorange differences are shown in Figure 1. In both simulated and real tests, the user is repeating the same trajectory describing a square: for this reason double differences oscillate periodically. From Figure 1 it can be noted that real measurements are affected by a time-varying, device dependent, bias that is difficult to estimate. This effect is probably due to a lack of synchronization between reference and rover receivers: synchronization errors affect measurement generation and time-stamping.

Although this issue is still under investigation, the problem is probably inherent to the system and the environment selected for the tests. Multipath and fading are probably causing significant problems to the synchronization process highlighting one of the limitations of indoor synchronous navigation.

3. ASYNCHRONOUS RSS POSITIONING

In order to overcome the limitation detailed above, the asynchronous approach developed in [2] was adopted. In this case, the user position is determined by minimizing the error func-

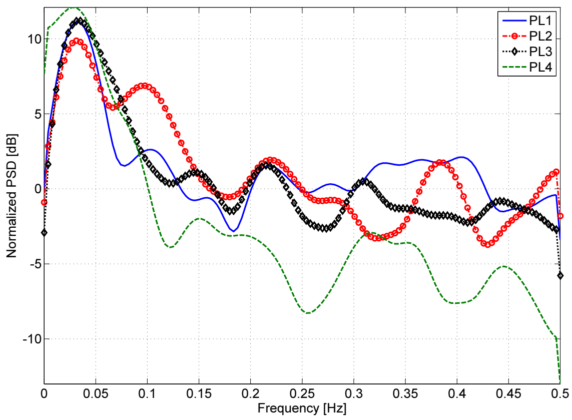

Fig. 2. PSDs of C/N_0 measurements (after DC removal) from four pseudolites placed in the corners of a large meeting room. The user circled around the large table placed in the middle of the room.

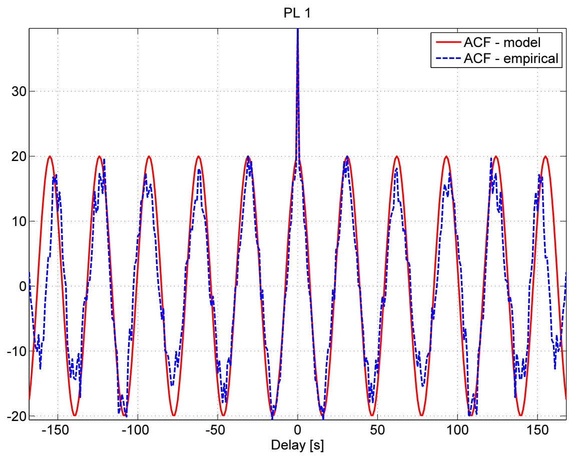

Fig. 3. Theoretical and empirical ACF of C/N_0 measurements from a single pseudolite. The user is performing a periodic activity which is reflected in the periodic behavior of the ACF.

tion

$$J(x, y) = \sum_{i=0}^{N-1} \left(\frac{C}{N_0}\right)_i E_i^2 \tag{5}$$

where

$$E_i = \left[\left(\frac{C}{N_0}\right)_i - K_i + \frac{1}{2}\alpha 10 \log_{10}\left[(x - x_i)^2 + (y - y_i)^2\right]\right] \tag{6}$$

is the difference between measured and predicted C/N_0 measurements. C/N_0 values are expressed in dB-Hz and are predicted using the empirical model [5]

$$\left(\frac{C}{N_0}\right)_i = K_i - \alpha 10 \log_{10}(d_i) \tag{7}$$

where α is the path-loss exponent, K_i is a constant accounting for the transmitted power and the noise floor, N_0. d_i is the distance between the receiver and the ith pseudolite. N is the number of C/N_0 measurements available and each term in the summation in (5) is weighted by its C/N_0.
This approach assumes the knowledge of the parameters

$$\alpha, K_i \quad \text{for } i = 0, ..., N-1.$$

These parameters are however unknown and have to be determined using a calibration process. This process was performed by exploiting the knowledge of several control point positions and their distances from the pseudolites. Using this approach, it was finally possible to perform indoor location using C/N_0 measurements.

4. PRE-FILTERING TECHNIQUES

In order to improve the performance of the RSS algorithm, a pre-filtering stage was introduced. In order to design a filter effectively improving the quality of C/N_0 measurements, a preliminary analysis in the frequency and correlation domains has been performed. Note that C/N_0 measurements are characterized by a Direct Current (DC) component which is determined by the average received power and the noise floor. The DC components of the C/N_0 measurements define a geometric point which can be thought as a reference location with respect to which the user is moving. For the analysis, the DC terms have been removed in order to better study the characteristics of the zero mean components which determine the relative displacement of the user.
The Power Spectral Densities (PSD) of the C/N_0 measurements (after DC removal) are shown in Figure 2 for four pseudolites placed in the corners of a large meeting room (about 10×7 m). During the test the user circled around the large table placed in the middle of the room with an almost constant speed. From Figure 2, it emerges that the PSD are characterized by a main peak at about 0.031 Hz corresponding to a periodicity of about 32 s, the average time required by the user to perform a loop. In addition to this, most of the power in Figure 2 is attenuated by more than 10 dB for frequencies higher than 0.15 Hz. This fact suggests that high frequency components can be removed with a cut-off frequency $f_c = 0.15$ Hz.
The Auto-Correlation Function (ACF) of the C/N_0 measurements from one of the pseudolites considered in Figure 2 is shown in Figure 3. The user is performing a periodic activity which is reflected in the periodic behavior of the ACF. From Figure 3, it is possible to isolate two parts: an impulsive term corresponding to the noise ACF and an oscillatory component determined by the user motion. This observation has been used to derive models for the ACFs of the C/N_0 noise and signal components. In turn, these models have been used in the design of a Wiener filter [6].
In addition to the considerations derived from the PSD and ACF analysis the following requirements have been identified

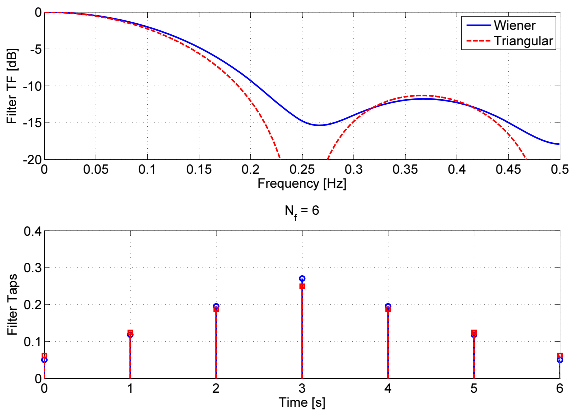

Fig. 4. TF and impulse responses of the filters used to pre-process C/N_0 measurements.

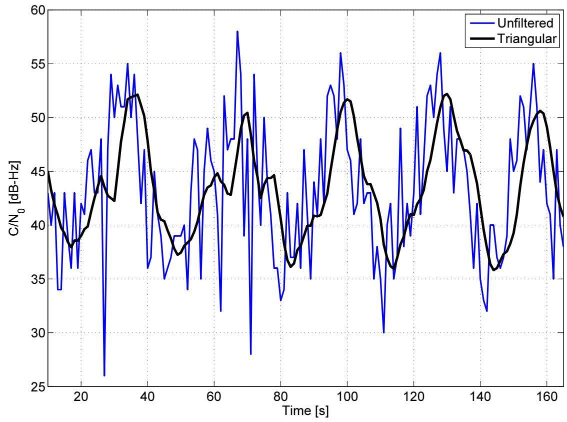

Fig. 5. Impact of triangular filtering of C/N_0 measurements. High-frequency noise components are effectively removed by the pre-filtering stage.

for the filter design:

- the filter should have a short impulse response: C/N_0 measurements are time-varying and long impulse responses may introduce significant biases due to the averaging of signals which are only locally stationary
- it has been empirically verified that symmetric impulse responses provide better results and thus should be adopted. The requirement of having short impulse responses limits the delay introduced by the filter.

The results reported above have been used to design a Finite Impulse Response (FIR) Wiener filter for the pre-processing of C/N_0 measurements. The Transfer Function (TF) of the filter is depicted in Figure 4 along with its impulse response. The filter mainly preserves low frequency components as desirable from the PSD analysis. The short impulse response selected (7 samples) is sufficient to significantly improve the algorithm performance, as detailed in Section 5, without introducing significant delays.

By inspecting the impulse response of the Wiener filter, it was found that it can be effectively approximated by a triangular function. This fact is highlighted in Figure 4 where the impulse responses and TFs of the two filters are compared. Their good agreement suggests the usage of a filter with a triangular impulse response which is simpler to design for different filter lengths. The effect of triangular filtering can clearly seen in Figure 5 which shows filtered and unfiltered C/N_0 measurements. High-frequency noise components are effectively removed by the pre-filtering stage.

5. EXPERIMENTAL RESULTS

In order to demonstrate indoor navigation using asynchronous pseudolitesystem, several data collections were conducted. Although different environments were considered, the case of a large meeting room is presented in the following. Similar results were obtained for the other environments considered. Four pseudolites were used and placed in the corners of the room, the measurement unit was composed by a LEA-6T u-blox receiver with a patch antenna. The receiver was connected to an Andorid mobile phone. During the first phase of the tests, several control points were placed in the meeting room; their locations were carefully determined by surveying the room and for each control point data were collected and used to calibrate the system. Then the calibrated model was used to demonstrate indoor navigation in *repeatability tests*. During these tests, the user performed several loops around a large table present in the meeting room trying to repeat always the same trajectory. The quality of the navigation solution was assessed by comparing the different trajectories estimated for the different loops. A high consistency level of the navigation solution indicates the good performance of the system.

A comparison among the solutions obtained applying triangular (red dashed line) and Wiener (blue line) filtering is provided in To this end in Figure 6. The solution using unfiltered measurements is also plotted (black dashed line) as comparison term. The solutions are plotted in a local reference frame with the origin in the upper left corner of the room and the axes oriented along the East and North directions. Both filtering techniques provide significant improvements with respect to the unfiltered solution. The trajectory followed by the user clearly emerges from the filtered solutions. Although the user locations are inside the room, it is not possible to identify the user trajectory from the solution obtained using unfiltered measurements. No significant differences can be appreciated between the two solutions with filtered measurements. Thus only the filter with triangular impulse response is further considered. The navigation solution estimated for five subsequent loops is provided in Figure 7. The trajectories estimated for the five laps is very consistent and only slight differences (sub-metre level) between the different laps

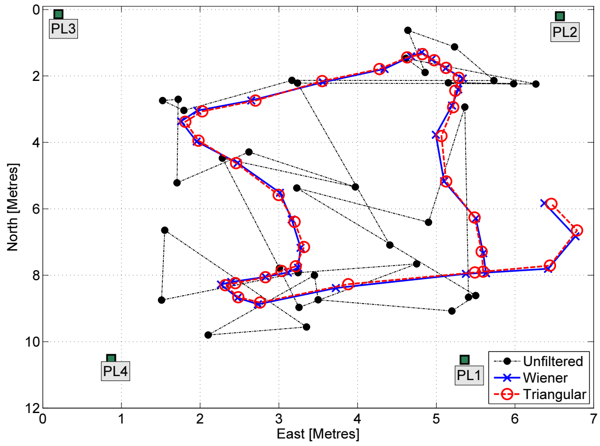

Fig. 6. Comparison between the navigation solutions obtained using the Wiener and triangular filters used for smoothing C/N_0 measurements. The navigation solution obtained using unfiltered measurements is also provided as a term of comparison. Loop performed in a large meeting room.

can be noted, demonstrating the high repeatability and consistency of the test. Only a slight degradation of the position was appreciated during the third lap due to the loss of lock on the signal of pseudolite3. The error was however within few metres demonstrating the robustness of the algorithm developed which was able to provide reliable solutions using only three pseudolites.

6. CONCLUSIONS

In this paper, the problem of indoor navigation using pseudolites was addressed. In particular, two types of pseudolite technologies, synchronous and asynchronous systems, were considered. The limitations of synchronous pseudolite systems were analyzed and it was shown that multipath and other propagation impairments can significantly prevent the system from achieving the level of synchronization required for determining travel time measurements.

On the contrary indoor navigation with metre level accuracy was demonstrated using C/N_0 measurements and an empirical propagation model. The performance of the system can be greatly improved using a pre-filtering stage for smoothing C/N_0 measurements the properties of which were analyzed and exploited for the filter design.

The use of asynchronous pseudolites significantly reduces the design and implementation constraints of the system: the different devices can operate independently and the system can be implemented in frequency bands different from the GNSS frequencies since inter-frequency biases are no longer relevant.

Finally, the performance of indoor navigation systems can be significantly degraded by poor geometries and interference

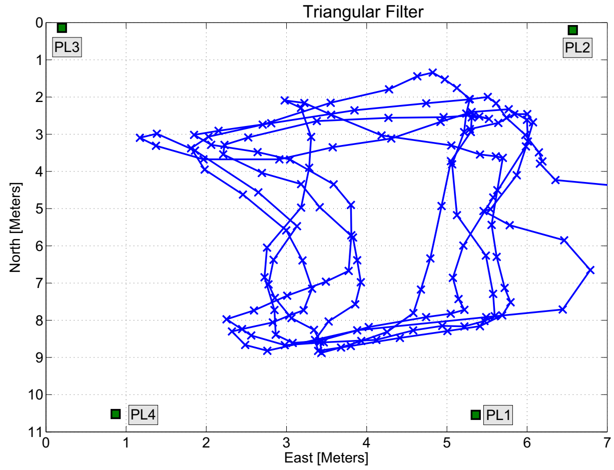

Fig. 7. Position estimates obtained using the RSS asynchronous technique and processing filtered C/N_0 measurements. Triangular filter, repeatability tests.

problems: map-based constraints and information on the user dynamics should be exploited to further improve the accuracy of the navigation solution.

REFERENCES

[1] H. Laitinen and M. Ström, "Single-frequency carrier navigation in a synchronised pseudolite network," in *Proc. of the European Navigation Conference ENC-GNSS*, Naples, Italy, May 2009, pp. 1–8.

[2] D. Borio and C. Gioa, "Indoor navigation using asynchronous pseudolites," in *Proc. of the 6th European Workshop on GNSS Signals and Signal Processing*, Institute of Space Technology and Space Application. Universit at der Bundeswehr M unchen, Germany, Dec. 2013, pp. 1–8.

[3] Space System Finland, *User's Manual Pseudolite Navigation System*, Mar. 2010.

[4] E. D. Kaplan and C. Hegarty, Eds., *Understanding GPS: Principles and Applications, Second Edition*, 2nd ed. Artech House, November 2005.

[5] Y. Okumura, E. Ohmori, T. Kawano, and K. Fukuda, "Field strength and its variability in vhf and uhf land-mobile radio service," *Review of the Electrical Communication Laboratory*, vol. 16, no. 9-10, pp. 825–873, 1968.

[6] S. Haykin, *Adaptive Filter Theory*, 4th ed. Prentice Hall, Sep. 2001.